

Controlled Growth of Nanoparticle Clusters through Competitive Stabilizer Desorption**

Jacek K. Stolarczyk, Swapankumar Ghosh, and Dermot F. Brougham*

Suspensions of superparamagnetic nanoparticles, or magnetic fluids, have found many applications, perhaps most importantly in biomedicine as drug delivery platforms^[1] that can be triggered thermally or by electronic pulses,^[2] as actuators to manipulate and control cell function,^[3] and as mediators for hyperthermia.^[4] Because of their magnetic moments, it is possible to localize the particles in the body by using externally applied magnetic fields, and to detect their presence either by magnetometry,^[5] or by magnetic resonance imaging (MRI).^[6] MRI is the field in which these materials have found the most important applications as they offer significant advantages of strong and tunable^[7] image contrast.

The properties of nanoparticles (NPs) and their suspensions are very strongly size-dependent, as a result there are many reports of different approaches to the control of NP size.^[8] In the field of bionanotechnology, nanoparticle clusters (NPCs) are often used to amplify the capabilities of the primary NPs (typically 5–15 nm in size), while maintaining the advantages that arise from the nanoscale dimensions of the clusters. Control of NPC size within the range of 20–400 nm can also improve their biodistribution and can help target the agent to specific structures, for instance, the porous vasculature of solid tumors can be targeted by objects that are approximately 150 nm in size. For applications as contrast agents in MRI, magnetic NPCs exhibit higher magnetization than dispersed primary NPs, which is important for contrast generation. The clusters can also remain superparamagnetic, a characteristic of the small primary NPs that increases colloidal stability. Nanoparticulate contrast agents for non-

gastrointestinal imaging include Endorem, which has a broad size distribution, and Sinerem (cluster size 50 nm), which is formed by fractioning Endorem suspensions. This improvement in size facilitates the use of Sinerem in MR-angiography and vascular staging of reticuloendothelial system (RES)-directed liver diseases. An important advantage of NPCs is the potential to tune their properties by controlling interactions between NPs. Berret et al.^[9] have reported the preparation of clusters of superparamagnetic γ -Fe₂O₃ NPs with cationic–neutral copolymers and have identified their potential as negative contrast agents, which arises from strong interparticle interactions.

Methods for preparing magnetic NPCs include the reaction of primary NPs with polymers.^[9,10] This approach can give some control over the cluster size, however, for a given polymer, stable suspensions can only be produced at one cluster size, and larger clusters are associated with low NP loading. An alternative approach is in situ NP formation^[10,11] in the presence of polymers. In some cases the cluster size can be controlled, though it was demonstrated that loading-dependent properties, and usually the cluster size, are very sensitive to the reaction conditions used. Thus there is a requirement for a general approach to the production of clusters of selectable size, in particular those composed of magnetic NPs.

Herein, we report the preparation of stable non-aqueous oleic acid (OA) stabilized magnetic fluids by suspending preformed solid NPs, and subsequent in situ NPC growth and stabilisation. The clusters were characterized by dynamic light scattering (DLS), transmission electron microscopy (TEM), and NMR relaxation time analysis, which provide information on the size and magnetic properties of the clusters and their stability. The process produces a gradual increase in the mean size of the suspended population of particles, because of the ongoing growth of NPCs and concurrent depletion of the suspension of dispersed NPs. In this way, the size distribution of the suspension remains monodisperse throughout the growth phase and the loading density of the clusters remains constant. Critically, the process can be stopped at any time and restarted by the operator, which makes it possible to produce NPCs with precise size selection and also offers the potential for further synthetic innovation. Thus, the process has potential for application in the growth of many types of size-controlled NPCs. Materials of this type may find applications for biomedical targeting, given recent advances in phase-transfer chemistry,^[12] or in other technologies.

The cluster growth experiments were performed in a UV cuvette with 50.0 mg of cyanopropyl-modified silica particles ((50 ± 20) μ m, Alltech Associates) that formed a thin layer at the bottom. Subsequently, a dispersion of 15 nm primary iron

[*] Dr. J. K. Stolarczyk, Dr. S. Ghosh,^[†] Dr. D. F. Brougham
School of Chemical Sciences, Dublin City University
Glasnevin, Dublin 9 (Ireland)
Fax: (+353) 1700-5503
E-mail: dermot.brougham@dcu.ie

Dr. D. F. Brougham

National Institute for Cellular Biotechnology, Dublin City University
Glasnevin, Dublin 9 (Ireland)

[†] Current address:
National Institute for Interdisciplinary Science & Technology, CSIR
Trivandrum 695019 (India)

[**] This work was supported by the Enterprise Ireland Proof of Concept Fund (PC/2006/207). J.S. also acknowledges Science Foundation Ireland (MASF666). We thank Carla Meledandri for assistance with many of the methods used in this research. We acknowledge Dr. David Cottell, Electron Microscopy Laboratory, University College Dublin, for access to TEM facilities, and also Sean Quilty (Particular Sciences) and Dr. Mike Kaszuba (Malvern) for advice on the DLS measurements.



Supporting information for this article is available on the WWW under <http://dx.doi.org/10.1002/anie.200803895>.

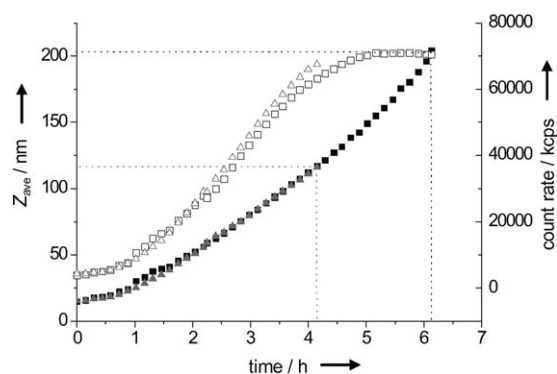


Figure 1. Growth of clusters of iron oxide NPs observed by DLS; Z_{ave} (filled squares and triangles) and corresponding backscattered light intensity (open squares and triangles) for two samples placed over CN-modified silica (50.1 mg). Growth was stopped when the Z_{ave} value reached 120 nm (gray triangles) and 200 nm (black squares). The process is reproducible between runs when care is taken to recreate the same starting conditions.

oxide NPs (1.2 mL of a 7.4 mM dispersion in heptane) was carefully placed in the cuvette to avoid agitating the silica. Figure 1 shows the average hydrodynamic diameter, Z_{ave} ,^[13] of the particles in the dispersion (derived from DLS measurements, see the Supporting Information). The Z_{ave} value increased to 200 nm over 6 hours after exposure to silica, while retaining a constant low polydispersity index (PDI) of (0.20 ± 0.01) . Over the same time period, 53% of the iron oxide precipitated and the Fe concentration decreased from 7.4 to 3.4 mM. After about 4 hours, the precipitation rate increased, as evidenced by the inflection in the backscattered light intensity. The clusters continued to grow, but the PDI value gradually increased to 0.29 after 6 hours.

The DLS size distributions show that the growing NPC suspensions are monodisperse, with very few small particles remaining (Figure 2). The growth process can be stopped by removing the dispersion from contact with the silica particles. This allowed us to produce dispersions of clusters with a Z_{ave}

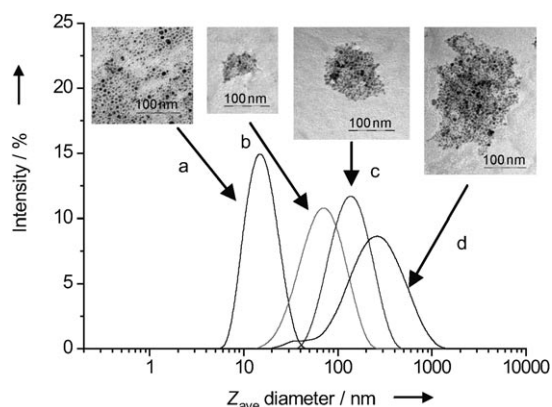


Figure 2. Size distribution profiles obtained from the DLS intensity data following the growth of the clusters for a) initial $Z_{\text{ave}} = 15.0$ nm primary NPs ((17.8 ± 6.5) nm), b) $Z_{\text{ave}} = 60$ nm clusters ((82 ± 35) nm), c) $Z_{\text{ave}} = 120$ nm clusters ((157 ± 58) nm), and d) $Z_{\text{ave}} = 200$ nm clusters ((287 ± 110) nm), each with corresponding TEM images. The mean and σ values given in brackets were obtained from log-normal-distribution fits to the distribution profiles shown above.

size equal to 60, 120, and 200 nm, and to inspect them using a JEOL 2000 TEM (see Figure 2 and the Supporting Information). The micrographs demonstrate that the increase in the average size is due to the formation of clusters of NPs rather than growth of the primary particles by Ostwald ripening or related processes,^[14] that is, the size of the primary NPs did not change.

The image contrast is strongly influenced by the molar NMR spin-lattice relaxation rate enhancement of the suspending solvent, because of the presence of the magnetic agent. This factor, termed the relaxivity, has units of $\text{s}^{-1}\text{mM}^{-1}$ (Fe concentration). Thus the spin-lattice relaxivity, r_1 is given by Equation (1):

$$r_1 = \frac{R_{1,\text{obs}} - R_{1,\text{dipolar}}}{[\text{Fe}]} \quad (1)$$

where $R_{1,\text{obs}}$ is the measured solvent relaxation rate ($1/T_{1,\text{obs}}$), and $R_{1,\text{dipolar}}$ is the observed rate in the absence of a superparamagnetic enhancement. Typical values of r_1 for NP dispersions are in the range $10\text{--}20 \text{ s}^{-1}\text{mM}^{-1}$ for clinical MRI fields of 60–100 MHz.^[6a] The magnetic field dependence of the relaxation rate can be measured in the range 0.25 mT to 0.5 T, which is equivalent to the ^1H resonance frequency range of 0.01–20 MHz, by using the technique of nuclear magnetic resonance dispersion, NMRD.^[15] The profiles obtained are commonly used to investigate the properties of magnetic colloidal dispersions, which are known to determine the MRI response.^[16,17]

The NMRD profiles of the heptane dispersions are shown in Figure 3. The profile of the primary NP suspension shows the expected shape and clearly conforms to the well-described behavior for aqueous suspension of superparamagnetic iron oxide NPs.^[17,18] Despite the formation of clusters, the NPC suspensions retain this characteristic superparamagnetic signature. The position of the high-frequency maximum r_1 value remains almost unchanged, but there is a slight attenuation of the dispersion in the mid-frequency range because of increased effective anisotropy energy.^[17] We attribute this to weak interparticle interactions within the NPCs, which nevertheless remain superparamagnetic, even at a cluster size of 200 nm.

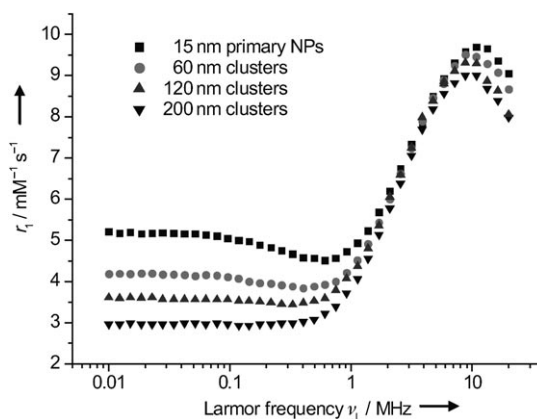


Figure 3. ^1H relaxation profiles, recorded at 298 K in heptane, for dispersions of primary NPs and NPCs.

The dispersions of primary NPs that we have produced are completely stable for periods of months. The cause of NPC growth is the presence of the competing phase, silica. As mentioned above, there is a gradual loss of iron oxide from the suspension over the course of the experiment. This is confirmed by the observation of a film of iron oxide on the surface of the silica by the end of the experiment, and by a marked increase in transmission of light through the sample. We have also demonstrated that the presence of the substrate is an ongoing requirement for continuation of the process. Figure 4a shows that cluster growth ceases within less than 3 minutes of the suspension being removed from contact with the silica, in this case the sample was removed when the Z_{ave} value reached 58 nm. In fact, by using NMRD and DLS we have shown that suspensions produced in this way, with Z_{ave} values of up to 120 nm, are stable and remain unchanged for periods of weeks. Re-exposure of the same sample to fresh silica resulted in the recommencement of cluster growth, although with a different rate than in the earlier phase. The change in the kinetics reflects different reaction conditions on restarting the process.

The role of the CN-modified silica is clearly to generate NPs activated towards interaction. In separate experiments, we have shown that this type of silica depletes heptane solutions of OA over a timescale of several hours (see the Supporting Information). This is expected, as the porous (60 Å size) silica we have used is designed for solid-phase extraction of polar molecules in nonpolar solvents. Thus, activated NPs could be generated without direct contact of the particles with the silica, by depletion of OA from the medium, altering the equilibrium between iron oxide bound and free surfactant (Figure 5). The concentration of activated particles that could be produced by this process is probably extremely low, given that OA is chemisorbed onto the iron oxide surface. However, at defect sites on the NP surface, the thermodynamics of binding could be significantly different, and could give rise to the small number of open sites.

The possibility of producing activated NPs from direct contact, by temporary adsorption of the NPs on silica and subsequent desorption of activated NPs, should also be

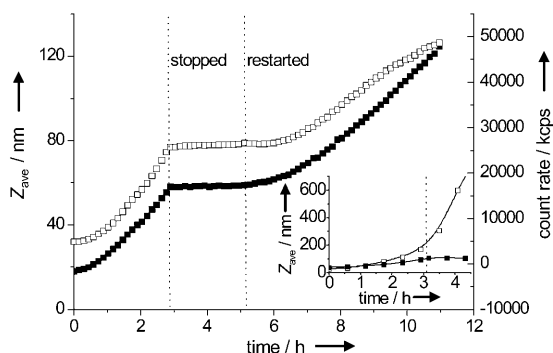


Figure 4. Controlled growth experiment stopped at 3 h by removing the dispersion from the CN-modified silica and restarted again by placing the dispersion over fresh silica; size (filled squares) and corresponding intensity (open squares). The inset shows a growth experiment stopped at 3 h by addition of two drops of OA into the cuvette (filled squares) and a similar experiment which was allowed to proceed undisturbed (open squares).

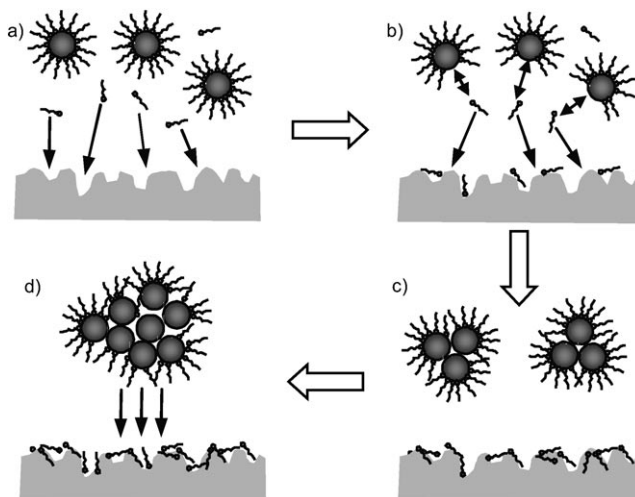


Figure 5. a) Depletion of OA, b) desorption of OA from the NPs and their destabilization, c) formation of clusters, and d) growth of clusters and their partial precipitation.

considered. Van Ewijk and Philipse reported that attraction between fatty-acid-coated magnetite NPs and a stable colloid of octadecanol-coated silica spheres of 420 nm in nonpolar solvents led to gradual coating of the silica particles over hundreds of hours.^[19] Critically, the process was shown to be irreversible in nonpolar media; desorption could only occur upon transfer to a solvent with a higher dielectric constant. It is unlikely, therefore, that a similar process is responsible for generation of activated NPs in suspension, in the case of the $\text{Fe}_3\text{O}_4/\text{OA}/\text{heptane}/\text{silica-CN}$ system. However, a significant fraction of the NPs and clusters clearly bind irreversibly to, or precipitate on, the silica surface over the course of NPC growth up to 200 nm.

The underlying principle of the cluster growth process is that the substrate generates a small subpopulation of NPs that are partially depleted of their stabilizer coating, and hence are activated with respect to interaction with other NPs or NPCs. We have shown that the introduction of further quantities of OA at any time permanently arrests the growth of suspensions left in contact with silica by blocking adsorption sites on both solid phases (Figure 4b). This approach can also be used to stabilize NPC suspensions at any stage of the growth, that is, when the NPCs are of any size. We conclude that, during the growth phase, the concentration of activated particles is low and is continuously replaced through the action of the substrate. This is supported by the slow growth rate and its cessation on removal of the substrate or the addition of a very small quantity of OA.

Most instructive however, is the very sensitive dependence of the growth rate and characteristics on the relative quantities of iron oxide to substrate used. If the iron concentration is too low, or the quantity of silica used significantly increased, normal destabilization and precipitation is observed, with a rapid increase in the Z_{ave} value together with an increase in the PDI value to 0.5–1.0 (very polydisperse), and with an increase in the backscattered light intensity because of the presence of larger particles. A maximum in the intensity is observed within 1 hour, followed by a collapse as the remaining aggregates precipitate and a

clear, colorless liquid remains. On the other hand, under the conditions for controlled NPC growth identified for the $\text{Fe}_3\text{O}_4/\text{OA}/\text{heptane}/\text{silica-CN}$ system, unimodal size distributions are maintained during the gradual growth phase as the smaller bodies in the distribution remain more active. We interpret the inflection that is clear at about 100–150 nm (Figure 1) as a transition from an initial phase where cluster growth arises solely from the addition of NPs to a later phase where clusters combine. We will present a detailed investigation into the mechanism and kinetics of controlled cluster growth, and the role of the substrate in maintaining monodispersity of the growing cluster size distribution in a forthcoming report.

The essential components of the NPC growth process, exhibited by $\text{Fe}_3\text{O}_4/\text{OA}/\text{heptane}/\text{silica-CN}$, are not necessarily specific to that particular system. The conditions for competitive stabilizer desorption leading to controlled cluster growth could, in principle, be identified for a wide range of NPs that are stabilized by many surface-active species and that are dispersed in many solvents. For instance, we have produced similar clusters with good monodispersity at slightly different concentrations (for $\text{Fe}_3\text{O}_4/\text{OA}$ in heptane over C18-grafted silica, see the Supporting Information). The key step in adapting the process for any given stabilized NP suspension is identifying appropriate substrates and reaction conditions for competitive desorption.

The growth process presented herein therefore has the potential to address the two main problems in the production of NPCs. Firstly, the good control over the cluster size distribution we have demonstrated may lead to better-defined properties, including magnetization, particle loading, and drug release rate. Secondly, with our approach, the final NPC size can be selected by continuous monitoring of the growth. This allows production of NPCs over a wide size range, with constant loading density, for different applications or further derivatization.

Experimental Section

Primary superparamagnetic iron oxide NPs were synthesized by alkaline co-precipitation of Fe^{II} and Fe^{III} salts following a modification of the procedure published by Shen et al.^[20] FeCl_2 (0.43 mmol) and FeCl_3 (0.86 mmol) were dissolved in deionised water (20 mL) and heated to 80 °C under an N_2 atmosphere. OA (0.39 mmol) was added dropwise, followed by NH_4OH (28 % w/w, 0.7 mL). The iron oxide NPs were separated by using a magnet, washed, dispersed in heptane, and any remaining aggregates were removed by centrifugation (for details see the Supporting Information). The procedure yielded a monodisperse and stable dispersion of 15 nm NPs. The amount of OA represents only a modest excess (5:1) of the stabilizer with respect to available sites on the NP surfaces, if an average fatty-acid footprint of 23 \AA^2 is assumed.^[20]

Received: August 7, 2008

Published online: December 3, 2008

Keywords: fatty acids · iron · magnetic properties · nanostructures · superparamagnetism

- [1] a) M. K. Yu, Y. Y. Jeong, J. Park, S. Park, J. W. Kim, J. J. Min, K. Kim, S. Jon, *Angew. Chem.* **2008**, *120*, 5442–5445; *Angew. Chem. Int. Ed.* **2008**, *47*, 5362–5365; b) N. Kohler, C. Sun, J. Wang, M. Zhang, *Langmuir* **2005**, *21*, 8858–8864; c) T. Neuberger, B. Schöpf, H. Hofmann, M. Hofmann, B. von Rechenberg, *J. Magn. Mater.* **2005**, *293*, 483–496; d) C. Alexiou, R. Jurgons, R. J. Schmid, C. Bergemann, J. Henke, W. Erhardt, E. Huenges, F. Parak, *J. Drug Targeting* **2003**, *11*, 139–149.
- [2] a) M. Babincová, P. Čičmanec, V. Altanerová, Č. Altaner, P. Babinec, *Bioelectrochemistry* **2002**, *55*, 17–19; b) A. M. Derfus, G. von Maltzahn, T. J. Harris, T. Duza, K. S. Vecchio, E. Ruoslahti, S. N. Bhatia, *Adv. Mater.* **2007**, *19*, 3932–3936.
- [3] J. Dobson, *Nat. Nanotechnol.* **2008**, *3*, 139–143.
- [4] a) A. Jordan, R. Scholz, P. Wust, H. Fähring, R. Felix, *J. Magn. Mater.* **1999**, *201*, 413–419; b) S. Mornet, S. Vasseur, F. Grasset, E. Duguet, *J. Mater. Chem.* **2004**, *14*, 2161–2175; c) J.-P. Fortin, F. Gazeau, C. Wilhelm, *Eur. Biophys. J.* **2008**, *37*, 223–228.
- [5] a) B. S. Kim, J. M. Qiu, J. P. Wang, T. A. Taton, *Nano Lett.* **2005**, *5*, 1987–1991; b) E. V. Shtykova, X. Huang, N. Remmes, D. Baxter, B. Stein, B. Dragnea, D. I. Svergun, L. M. Bronstein, *J. Phys. Chem. C* **2007**, *111*, 18078–18086.
- [6] a) R. N. Muller, A. Roch, J.-M. Colet, A. Ouakssim, P. Gillis in *The Chemistry of Contrast Agents in Medical Magnetic Resonance Imaging* (Eds.: A. E. Merbach, É. Toth), Wiley, New York, **2001**, pp. 417–435; b) R. Weissleder, M. J. Pittet, *Nature* **2008**, *452*, 580–589; c) C. Corot, P. Robert, J.-M. Idée, M. Port, *Adv. Drug Delivery Rev.* **2006**, *58*, 1471–1504; d) E. X. Wu, H. Tang, J. H. Jensen, *NMR Biomed.* **2004**, *17*, 478–483; e) M. Brähler, R. Georgieva, N. Buske, A. Müller, S. Müller, J. Pinkernelle, U. Teichgräber, A. Voigt, H. Bäumler, *Nano Lett.* **2006**, *6*, 2505–2509.
- [7] Y.-M. Huh, Y.-W. Jun, H.-T. Song, S. Kim, J.-S. Choi, J.-H. Lee, S. Yoon, K.-S. Kim, J.-S. Shin, J.-S. Suh, J. Cheon, *J. Am. Chem. Soc.* **2005**, *127*, 12387–12391.
- [8] a) A. H. Lu, E. L. Salabas, F. Schüth, *Angew. Chem.* **2007**, *119*, 1242–1266; *Angew. Chem. Int. Ed.* **2007**, *46*, 1222–1244; b) S. Sun, H. Zeng, *J. Am. Chem. Soc.* **2002**, *124*, 8204–8205; c) S. Wan, J. Huang, H. Yan, K. Liu, *J. Mater. Chem.* **2006**, *16*, 298–303.
- [9] J.-F. Berret, N. Schonbeck, F. Gazeau, D. El Kharrat, O. Sandre, A. Vacher, M. Airiau, *J. Am. Chem. Soc.* **2006**, *128*, 1755–1761.
- [10] A. Ditsch, P. E. Laibinis, D. I. C. Wang, T. A. Hatton, *Langmuir* **2005**, *21*, 6006–6018.
- [11] a) J. Ge, Y. Hu, M. Biasini, W. P. Beyermann, Y. Yin, *Angew. Chem.* **2007**, *119*, 4420–4423; *Angew. Chem. Int. Ed.* **2007**, *46*, 4342–4345; b) S. A. Corr, S. J. Byrne, R. Tekoriute, C. J. Meledandri, D. F. Brougham, M. Lynch, C. Kerskens, L. O' Dwyer, Y. K. Gun'ko, *J. Am. Chem. Soc.* **2008**, *130*, 4214–4215; c) S. A. Corr, Y. K. Gun'ko, R. Tekoriute, C. J. Meledandri, D. F. Brougham, *J. Phys. Chem. C* **2008**, *112*, 13324–13327.
- [12] T. Zhang, J. Ge, Y. Hu, Y. Yin, *Nano Lett.* **2007**, *7*, 3203–3207.
- [13] International Standard ISO13321, Methods for Determination of Particle Size Distribution Part 8: Photon Correlation Spectroscopy, ISO, **1996**.
- [14] I. M. Lifshitz, V. V. Slyozov, *Phys. Chem. Solids* **1961**, *19*, 35–50.
- [15] R. Kimmich, E. Ansaldo, *Prog. Nucl. Magn. Reson. Spectrosc.* **2004**, *44*, 257–320.
- [16] E. Taboada, E. Rodríguez, A. Roig, J. Oró, A. Roch, R. N. Muller, *Langmuir* **2007**, *23*, 4583–4588.
- [17] A. Roch, R. N. Muller, P. Gillis, *J. Chem. Phys.* **1999**, *110*, 5403–5411.
- [18] C. J. Meledandri, J. K. Stolarczyk, S. Ghosh, D. F. Brougham, *Langmuir* **2008**, *24*, 14159–14165.
- [19] G. A. van Ewijk, A. P. Philipse, *Langmuir* **2001**, *17*, 7204–7209.
- [20] L. Shen, P. E. Laibinis, T. A. Hatton, *Langmuir* **1999**, *15*, 447–453.